

Semi-continuous gas and inorganic aerosol measurements at a boreal forest site: seasonal and diurnal cycles of NH_3 , HONO and HNO_3

Ulla Makkonen¹⁾, Aki Virkkula¹⁾²⁾, Heidi Hellén¹⁾, Marja Hemmilä¹⁾, Jenni Sund¹⁾, Mikko Äijälä²⁾, Mikael Ehn²⁾, Heikki Junninen²⁾, Petri Keronen²⁾, Tuukka Petäjä²⁾, Douglas R. Worsnop²⁾³⁾, Markku Kulmala²⁾ and Hannele Hakola¹⁾

¹⁾ Finnish Meteorological Institute, P.O. Box 505, FI-00560, Helsinki, Finland

²⁾ Department of Physics, FI-00014 University of Helsinki, Finland

³⁾ Aerodyne Research Inc., 45 Manning Rd, Billerica, MA 01821, USA

Received 31 Oct. 2013, final version received 17 Jan. 2014, accepted 10 Jan. 2014

Makkonen, U., Virkkula, A., Hellén, H., Hemmilä, M., Sund, J., Äijälä, M., Ehn, M., Junninen, H., Keronen, P., Petäjä, T., Worsnop, D. R., Kulmala, M. & Hakola, H. 2014: Semi-continuous gas and inorganic aerosol measurements at a boreal forest site: seasonal and diurnal cycles of NH_3 , HONO and HNO_3 . *Boreal Env. Res.* 19 (suppl. B): 311–328.

In a boreal forest environment at Hyttiälä (SMEAR II station), Finland, from 21 June 2010 to 31 April 2011, concentrations of gases (HCl , HNO_3 , HONO, NH_3 , SO_2) and inorganic ions (Cl^- , NO_3^- , SO_4^{2-} , NH_4^+ , Na^+ , K^+ , Mg^{2+} , Ca^{2+}) in PM_{10} and $\text{PM}_{2.5}$ particles were measured with an on-line ion chromatograph MARGA 2S. The MARGA data were compared with those of the filter samples and the Aerosol Mass Spectrometer. The linear-regression slopes derived from MARGA against the filter data were 0.98, 1.08, 0.50 and 1.31 for SO_2 , SO_4^{2-} , HNO_3 and NO_3^- , respectively. The respective coefficients of determination (r^2) were 0.89, 0.90, 0.70 and 0.93. After installing a concentration column, improved values of cation slopes of 1.00, 1.19, 0.88, 1.00, 0.73 and 0.89 for NH_3 , NH_4^+ , Na^+ , K^+ , Mg^{2+} , and Ca^{2+} , respectively, were obtained. The corresponding coefficients of determination (r^2) were: 0.79, 0.83, 0.95, 0.90, 0.85 and 0.62. According to these results, traditional filter collection can be replaced with the MARGA instrument at background sites, if a concentration column is used at least for the cations. This would improve the temporal resolution of the observations. The average concentrations of nitrogen-containing gases were highest in the summer (NH_3 : 0.47 ppb, HNO_3 : 0.10 ppb and HONO: 0.11 ppb), which can be explained by the higher temperatures and increased amounts of sunlight followed by stronger agricultural and soil-related sources. In the summer, clear diurnal cycles were found in all N-containing gases, but in the winter the concentrations remained low most of the time and no diurnal cycles were observed. The concentration of ammonia was found to depend exponentially on the prevailing temperature, the increase with temperature being strongest in dry conditions.

Introduction

Nitrogen-containing gases are important contributors to atmospheric processes and to the formation and growth of new particles. The concentrations of aerosol species, such as ammonium nitrate (NH_4NO_3), ammonium sulphate $[(\text{NH}_4)_2\text{SO}_4]$, ammonium bisulphate (NH_4HSO_4) and ammonium chloride (NH_4Cl), are strongly dependent on their gas-phase precursors, NH_3 , HNO_3 , SO_2 and HCl (Finlayson-Pitts and Pitts 2000, Kirkby *et al.* 2011). Ammonia (NH_3) is the most abundant gaseous base in the atmosphere and has a major role in neutralizing acids and in the formation of new particles (Kirkby *et al.* 2011, Kulmala *et al.* 2000). In the atmosphere, ammonia can also react slowly with the hydroxyl radical (OH), forming the amidogen radical (NH_2) which in turn reacts with nitrogen dioxide (NO_2) to form nitrous oxide (N_2O) (Park and Lin 1997), one of the main warming components in the atmosphere (Butterbach-Bahl 2011). Furthermore, nitric acid interacts with crustal and sea salt aerosol, forming calcium and sodium nitrate $[\text{Ca}(\text{NO}_3)_2]$ and NaNO_3 . The nitrogen-containing aerosols, as well as the sulphates, have a cooling effect on the climate through direct scattering of sunlight and through contribution to cloud formation (Sutton 2011). Nitrogen compounds participate both in the production and loss of the most important daytime atmospheric oxidant, the hydroxyl radical (OH). The dissociation of HONO contributes to the production of OH radicals (e.g. Kulmala and Petäjä 2011, Su *et al.* 2011). During the daytime OH radicals are consumed to form nitric acid in the reaction: $\text{NO}_2 + \text{OH}\cdot + \text{M} \rightarrow \text{HNO}_3 + \text{M}$ (Finlayson-Pitts and Pitts 2000).

There is still a lack of knowledge of the concentration of nitrogen-containing gases and their cycle in the ambient atmosphere (e.g., Su *et al.* 2011, Kulmala and Petäjä 2011), and until now no reliable semi-continuous measurements of ammonia have been performed in background areas of the Nordic countries. In this study, we measured gases and inorganic compounds in airborne particles with a 1-hour time-resolution using a commercially-available on-line ion chromatograph, MARGA 2S (The instrument for Measuring AeRosols and Gases in ambient Air; ten Brink *et al.* 2007), in a boreal forest. In the MARGA

instrument, gases are collected by diffusion in a wet rotating denuder (WRD) and for collecting aerosols this instrument takes the advantage of the principle of the Steam-Jet Aerosol Collector (SJAC) (e.g. Khlystov *et al.* 1995). In an earlier publication, the performance of the MARGA 2S instrument was evaluated in an urban environment (Makkonen *et al.* 2012, Rumsey *et al.* 2013). In a clean background environment in Europe, MARGA has previously been used at an EMEP (European Monitoring and Evaluation Programme) supersite in Scotland (Cape 2009). At the Finnish background stations, particles and inorganic gaseous compounds had earlier been measured with the EMEP filter-pack with a time resolution varying from 24 hours to several days (EMEP 2001, Ruoho-Airola *et al.* 2010). Using a semi-continuous instrument makes it possible to obtain data with short enough time resolution to characterize chemical processes, to evaluate models and to study sources, which would not be possible by using the traditional filter methods (Schaap *et al.* 2011, Aan de Brugh *et al.* 2012).

Concentrations of a suite of gases and aerosols were measured at a boreal forest measurement site in a large campaign, the “Hyttiälä United Measurements of Photochemistry and Particles in Air – Comprehensive Organic Precursor Emission Concentration 2010 (HUMPPA – COPEC-10)”, in July–August 2010 (Williams *et al.* 2011). The general goal of the campaign was to study the links between gas-phase oxidation chemistry and particle properties and processes. During the campaign, the MARGA instrument was used to measure water-soluble gases and inorganic compounds in particles, and it was left running at Hyttiälä to study seasonal variations and possible sources or sinks of nitrogen-containing gases.

The first goal of this study was to evaluate whether the MARGA instrument could be used to replace the EMEP filter method at the background stations with low concentrations. In addition, we compared the MARGA results with those from an Aerosol Mass Spectrometer (AMS) (Jayne *et al.* 2000, Jimenez *et al.* 2003) that provides the concentrations of the major aerosol constituents (organics, sulphate, nitrate, ammonium, and chloride) of submicron aerosols with a high time resolution.

The second goal of this work was to analyse the seasonal and diurnal cycles of nitrogen-containing trace gases NH_3 , HNO_3 and HONO. As explained above, these gases play an important role in atmospheric chemistry, yet their seasonal and diurnal cycles measured at our site with a high time resolution have not been presented before. The temperature dependence of ammonia will be compared with that found in other studies.

Material and methods

Measurement site

The measurements were carried out in Hyytiälä at the boreal forest research station SMEAR II (Station for Measuring Ecosystem–Atmosphere Relationships) from 21 June 2010 until 30 April 2011. The station ($61^\circ 51' \text{N}$, $24^\circ 17' \text{E}$) is situated in southern Finland, about 60 km NE of the city of Tampere. The station is surrounded by a coniferous Scots pine-dominated forest. A more detailed site description can be found in Hari and Kulmala (2005). The container in which the MARGA instrument was installed was air-conditioned and kept at a constant temperature of 20°C . The container was located in a small clearing about 5 m from the nearest trees. The inlet of the instrument was situated on the roof of the container at a height of 2.5 m above the ground. The time used in this study is local winter time (UTC + 2 hours).

MARGA

MARGA 2S ADI 2080 (Applikon Analytical BV, Netherlands) with two sample boxes was used in this study, in the same configuration as used in an earlier study in Helsinki (Makkonen 2012). Ambient air was drawn through a PM_{10} -inlet (Teflon coated impactor, URG-2000-30DBN-TC, $2 \text{ m}^3 \text{ h}^{-1}$) followed by a 50-cm-long polyethylene (PE) tube ($\varnothing 1.0''$) and divided into two flows, one going to the PM_{10} sample box through a 40-cm-long PE tubing ($\varnothing 0.5''$), while the other was directed through a 70-cm-long PE tube ($\varnothing 0.5''$) and $\text{PM}_{2.5}$ cyclone ($1 \text{ m}^3 \text{ h}^{-1}$ Teflon coated, URG-2000-30ENB) into the $\text{PM}_{2.5}$ sample box. In both compartments, the air was led through

a Wet Rotating Denuder (WRD) where water-soluble gases diffuse to the absorption solution (10 ppm hydrogen peroxide). Subsequently the ambient particles were collected in a Steam Jet Aerosol Collector (SJAC) (Slanina *et al.* 2001). Hourly samples collected in syringes were analyzed with a Metrohm cation and anion chromatograph using an internal standard (LiBr). The sample-stream was directed through the cation side to the anion IC and samples were injected simultaneously to both ICs. At the beginning of the measurements, cations were separated in a Metrosep C4 (100/4.0) cation column using $3.2 \text{ mmol l}^{-1} \text{ HNO}_3$ eluent. On 18 August 2010, the cation loop was replaced with a concentration column (Metrosep C PCC 1 VHC) and the HNO_3 eluent was replaced with a methane sulfonic acid eluent (2.1 ml MSA in 10 l water) to get a better baseline for nitrate. For anions a Metrosep A Supp 10 (75/4.0) column and a $\text{Na}_2\text{CO}_3/\text{NaHCO}_3$ ($7 \text{ mmol l}^{-1}/8 \text{ mmol l}^{-1}$) eluent was used. Gases (HCl , HNO_3 , HONO, NH_3 , SO_2) and inorganic ions (Cl^- , NO_3^- , SO_4^{2-} , NH_4^+ , Na^+ , K^+ , Mg^{2+} , Ca^{2+}) in the PM_{10} and in $\text{PM}_{2.5}$ particles were measured with the MARGA 2S. The instrument is described in more detail by Makkonen *et al.* (2012). For the data before 18 August 2010, field blanks of nitrate were subtracted from the initial NO_3^- and HNO_3 values, but other field blanks were close to the DLs. Approximately every three weeks the inlet tubes, WRDs and SJACs were replaced with clean ones or cleaned. The SJAC was cleaned in diluted HNO_3 in an ultrasonic bath, rinsed with ethanol and well rinsed with ultrapure water (Milli-Q conductivity $< 18 \mu\text{S cm}^{-1}$). The outer glass cylinder of WRD was detached and all the parts were washed with hot water, rinsed with ethanol and rinsed several times with ultrapure water to prevent any biological growth.

Filter sampling

The results from MARGA were compared with those of the EMEP filter-pack (EMEP 2001), which consists of three filters: the first is a Teflon filter for collecting particles, the second is a NaOH-impregnated cellulose filter (Whatman 40) for collecting SO_2 and HNO_3 , and the third is an oxalic-acid-impregnated cellulose filter

(Whatman 40) for collecting NH_3 . The sampling time (flow $1 \text{ m}^3 \text{ h}^{-1}$) was 2–3 days. The filters were extracted in ultrapure water (Milli-Q) and analysed by ion chromatographs (Waters and Dionex). The procedure is described in detail in the EMEP Manual (EMEP 2001). The averages of the corresponding time periods were calculated from the MARGA data and compared with the filter data.

AMS

The Aerodyne Aerosol Mass Spectrometer (AMS) measures aerosol particle chemical composition directly and quantitatively, using time-of-flight mass spectrometry (Jayne *et al.* 2000, Jimenez *et al.* 2003). An aerodynamic lens is used to focus aerosol particles of around 40–600 nm size (Liu *et al.* 2007) into a beam, and a thermal vaporization element at the temperature of 600 °C is used to flash-vaporize all non-refractory compounds in the sample, and electron impact ionization (EI) of 70 eV ionizes the formed sample gas. Finally, a time-of-flight mass spectrometer is used to produce a mass spectrum of the sampled aerosol particles and remaining carrier gas. The ambient aerosol concentration and composition is obtained using data inversion and analysis. The data is corrected for instrument collection efficiency (CE), which was unaffected by aerosol acidity related effects for most of the measurement period and was determined to be around 0.43.

The specific AMS used in this study features a compact time-of-flight (C-ToF) mass analyzer, the specifics of which are described by Drewnick *et al.* (2005). The particle time-of-flight (PToF) chamber was shorter than on a normal AMS, increasing ion signals at the expense of size-segregated chemistry measurements.

Results and discussion

Comparison of MARGA with independent methods

MARGA *versus* EMEP filter pack

The EMEP filter-pack samples were collected in

Hyttiälä with a sampling time of 2–3 days. Averages of the MARGA data were calculated for the same periods. Before the averaging, the zero-values found in the online data were replaced with $0.005 \mu\text{g m}^{-3}$. A linear regression (Fig. 1) MARGA *vs.* filter yielded slopes of 0.98 ($r^2 = 0.89$) and 1.08 ($r^2 = 0.90$) for SO_2 and SO_4^{2-} concentrations, respectively. For these compounds MARGA compared well also in the earlier studies in Helsinki, where the concentrations were higher, yielding slopes of 0.90 (MARGA *vs.* TEI 43iTL monitor) for SO_2 and 0.85 for SO_4^{2-} (Makkonen *et al.* 2012).

The concentrations of HNO_3 were clearly lower in MARGA than in the filter pack (slope 0.50, $r^2 = 0.70$), while the concentrations of NO_3^- were higher in MARGA than with the filter method (slope 1.31, $r^2 = 0.93$), yielding a regression slope of 0.97 ($r^2 = 0.89$) for the sum $\text{HNO}_3 + \text{NO}_3^-$. Based on this result and because of the sticky nature of HNO_3 , it is likely that a significant fraction of HNO_3 had been attached to the walls of the PE-tubing. This hypothesis is supported by the study of Rumsey *et al.* (2013): the regression analysis of HNO_3 concentrations of MARGA and the results of the denuder yielded slopes of 0.73 ($r^2 = 0.88$) and 0.57 ($r^2 = 0.88$). A better tubing material for collecting HNO_3 would have been perfluoroalkoxy Teflon, as recommended by Neuman *et al.* (1999). However, this is not a suitable material for collecting particles which are retained on Teflon walls by electrostatic forces. Furthermore, it is likely, especially on warm summer days, that the HNO_3 measured by Teflon filter was also underestimated: part of the NH_4NO_3 may have been volatilized from the Teflon front filters and moved to the next filters used for collecting gases. Because of these artifacts in the filter sampling, only the sums of $\text{HNO}_3 + \text{NO}_3^-$ and $\text{NH}_3 + \text{NH}_4^+$ are reported to the EMEP database (EMEP 2001).

The regression slopes of all the cations improved remarkably after removing the cation loop (500 μl) and installing the concentration column on 18 August 2010 (Fig. 2). The regression slopes with the ordinary loop and with the concentration column were 1.50 and 0.88, respectively, for Na^+ , 1.51 and 1.00 for K^+ , 3.39 and 0.73 for Mg^{2+} , 2.95 and 0.89 for Ca^{2+} and 1.23 and 1.19 for NH_4^+ . The coefficients

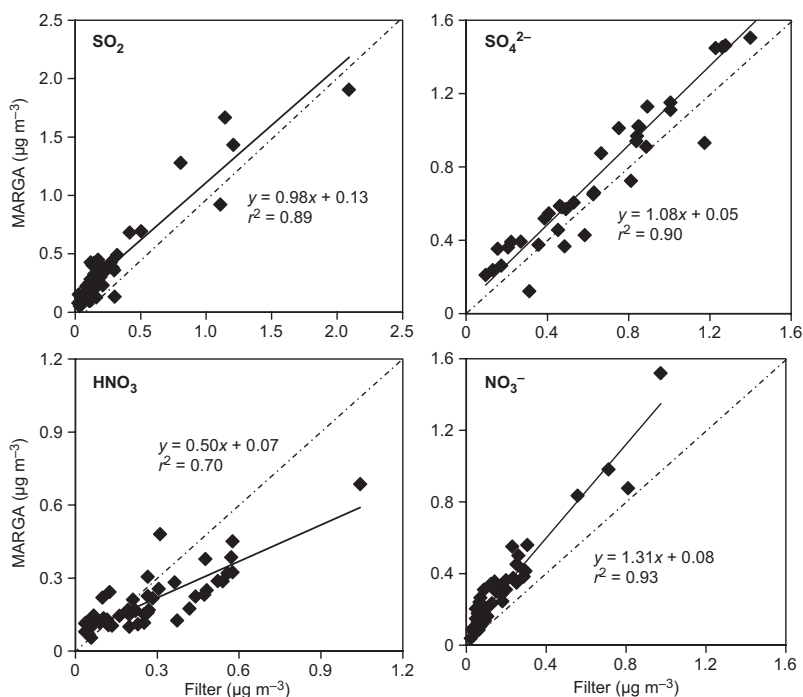


Fig. 1. Comparison of sulphur dioxide, sulphate, nitric acid and nitrate (with the PM₁₀ inlet) concentrations measured with MARGA with those analysed from the EMEP filter-pack samples.

of determination were also improved with the concentration column ($r^2 = 0.83\text{--}0.95$), except for Mg²⁺ ($r^2 = 0.85$) and Ca²⁺ ($r^2 = 0.62$) that had very low concentrations throughout the winter. Although the time resolution increases when an online instrument was used, we must also take into account that the measurement uncertainty increases at low concentrations. It must be noted that especially the cation peaks were often close or even under the official detection limits of MARGA.

MARGA versus AMS

The hourly-averaged AMS data were compared with the PM_{2.5} data of MARGA (Fig. 3). The sulphate concentrations measured with MARGA were in good agreement with those measured with AMS. The slope for the MARGA vs. AMS linear regression was 1.01 (intercept -0.25 , $r^2 = 0.92$), which indicates that sulphate was mainly in submicron particles. The MARGA ammonium data values were in general higher than those measured with AMS (slope 0.66, intercept -0.02), indicating that a considerable fraction of the ammonium was in particles larger

than 1 µm. For nitrate, there was not such a good an agreement between MARGA and AMS. The concentrations measured with AMS were often higher than those measured with MARGA. However, during the same period, the nitrate concentrations measured with MARGA were in good agreement with the EMEP filter data ($r^2 = 0.87$ and 0.93 for PM_{2.5} and PM₁₀, respectively). Nitrate concentrations were relatively low during the AMS measurement periods, which caused additional scatter. It is also possible that a slight offset may have arisen if the response to organic nitrates was lower in the MARGA and filter data compared with the AMS data. It should also be noted that the NO₃ blank which was subtracted from all the MARGA results may have not been constant during the whole measurement period and may have caused further inaccuracy.

Seasonal variations

The measurement data were divided into four classes by the season (Table 1). The season division was made according to prevailing temperatures (thermal seasons). On 15 August the temperature decreased from 19 °C to 14 °C and

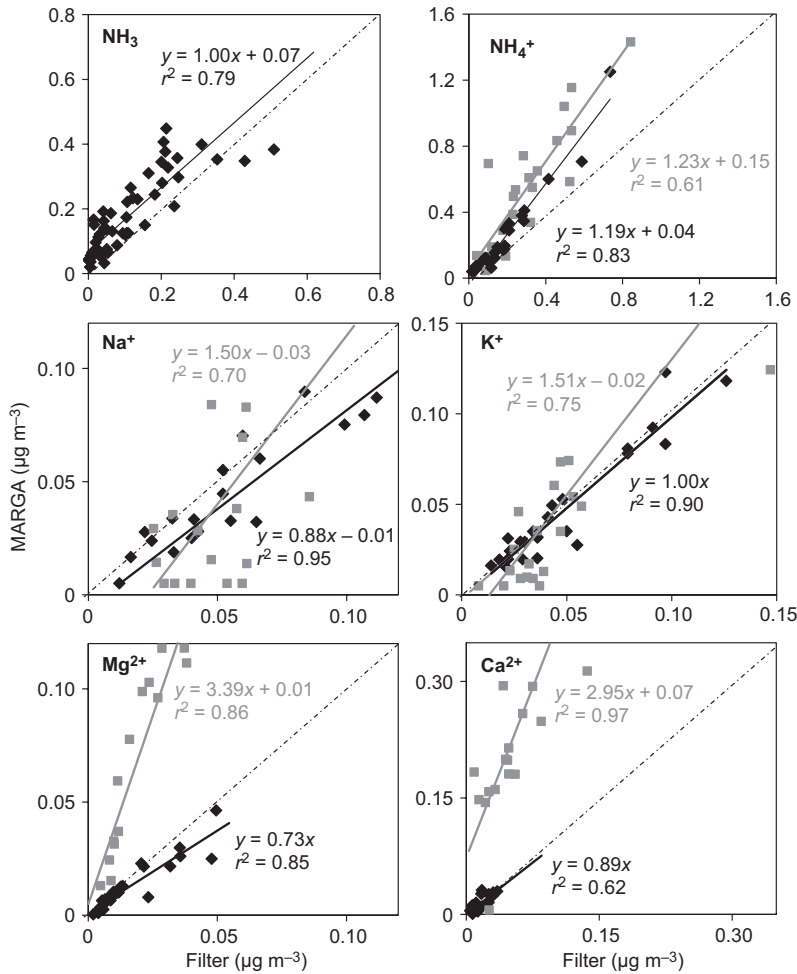


Fig. 2. Comparison of ammonia, ammonium, sodium, potassium, magnesium and calcium concentrations measured with MARGA with the PM₁₀ inlet with those analysed from the EMEP filter-pack samples. The concentrations obtained with MARGA were measured using an ordinary 500 µl cation loop (grey) and a cation pre-concentration column (black).

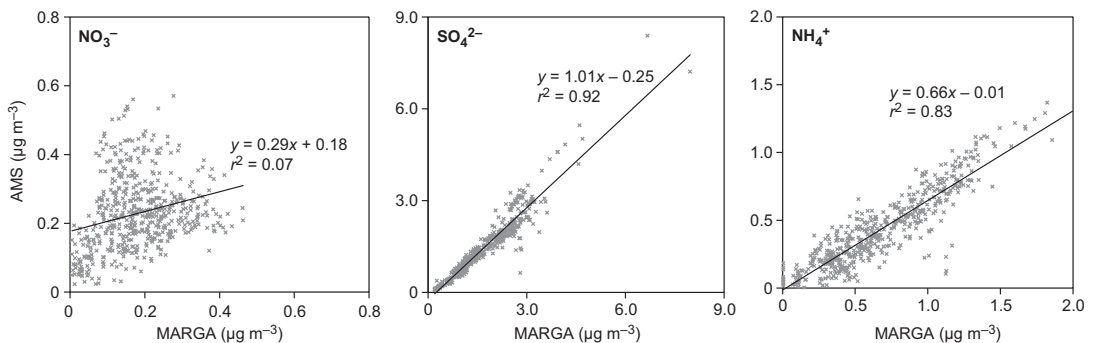


Fig. 3. Comparison of nitrate, sulphate, and ammonium concentrations measured with MARGA (using the PM_{2.5} inlet) with those measured with AMS. The cutoff diameter for the AMS is below 1.0 µm.

on 24 August it was already below 10 °C. In this analysis the autumn period was therefore defined as starting on 16 August. On 6 November the temperature dropped below 0 °C, starting the

winter period. On 4 March the daily average temperature rose above 0 °C for the first time, starting the spring period, although the temperature remained close to 0 °C for the rest of March

(Fig. 4). The ground was covered with snow (up to 0.75 m) from 8 November 2010 until late April 2011. Gaps in the measurement data were caused mainly by technical problems and maintenance operations.

In the winter, sulphur dioxide was the dominating trace gas (average 0.49 ppb; Table 2), whereas concentrations of all the nitrogen-containing gases were low (averages 0.05–0.07 ppb). The SO₂ concentration was elevated during a short, cold period (14–24 February 2011) when the daily average temperature remained below –20 °C (Fig. 4). The highest SO₂ concentration was measured during this period, 20 ppb on 18 February at 12:00. The simultaneously measured sulfate concentration in PM₁₀ was 0.13 μg m⁻³, which is less than the median concentration of 0.70 μg m⁻³ throughout the whole period discussed in this paper, which suggests that the origin of the observed high SO₂ concentrations was not a large-scale industrial source. In addition, back trajectories calculated with HYSPLIT (Draxler and Rolph 2013, Rolph 2013) show that air masses had come from the east-north-east and not over some of the largest SO₂ emitters in the Kola Peninsula. A possible source of SO₂ was the domestic heating with wood-burning stoves and oil burners — the period was cold, a situation which is often associated with strong inversions. Further meteorological analyses are omitted in this paper, however. Another indicator for domestic burning would be black carbon, which was also measured at SMEAR II. However, during February 2011 the black carbon instrument was out of order so it could not be used for confirming the source either.

The average HNO₃ concentration measured at Hyytiälä was at the same level (0.07 ppb) as the average concentration measured with MARGA in southeastern Scotland in 2007 (0.05 ppb; Cape 2009), but much lower than those measured at urban sites in Helsinki (0.13 ppb in winter and 0.22 ppb in spring; Makkonen *et al.* 2012). The highest seasonal average HNO₃ concentration, 0.10 ppb, occurred in summer, confirming that the formation of nitric acid requires nitrogen dioxide and solar radiation. High concentrations were occasionally observed also at the darkest time of the year. For instance, during an episode when winds blew over a

local sawmill about 5 km to the south-southeast of SMEAR II on 17–22 December, short NO₂ peaks as high as 25 ppb and HNO₃ peaks up to 0.38 ppb were detected, in addition to elevated monoterpene and aromatic hydrocarbon concentrations (Hakola *et al.* 2012).

The seasonal cycle of nitrous acid, HONO, was also very clear (Fig. 4). The highest concentrations were recorded in summer, which conforms with the observation that soil nitrite is a strong source of atmospheric HONO (Su *et al.* 2011). NO_x emitted by road traffic has been shown to be another important source of HONO. Kurtenbach *et al.* (2001) investigated the emissions and heterogeneous formation of HONO in a road traffic tunnel and found that the mean HONO-to-NO_x ratio was 0.008 ± 0.001. We operated the same MARGA instrument at the urban background SMEAR III site in Helsinki in 2009–2010 and found that most of the time there was at least as much HONO as the Kurtenbach *et al.* (2001) HONO-to-NO_x ratio predicts (Makkonen *et al.* 2012). From the measured ratios it was also deduced that traffic was not the only source of HONO at the urban site. The same approach is used here for the SMEAR II data. The HONO vs. NO_x concentrations, the latter obtained from the SMEAR II mast at the altitude of 8.4 m, clearly form two groups: in summer the ratio deviates by up to two orders of magnitude from the traffic ratio of Kurtenbach *et al.* (2001), suggesting possible HONO emissions from the boreal soil in line with the observations by Su *et al.* (2011). In the other seasons, the ratio was closer to the traffic ratio (Fig. 5). As in the urban data, HONO concentrations were very rarely smaller than those predicted by the NO_x concentration using the ratio by Kurtenbach *et al.* (2001).

There was a clear seasonal cycle in the ammonia and ammonium concentrations: they were

Table 1. Dates determining the four seasons.

Season	Period
Summer	22 June 2010–15 August 2010
Autumn	16 August 2010–5 November 2010
Winter	6 November 2010–3 March 2011
Spring	4 March 2011–30 April 2011

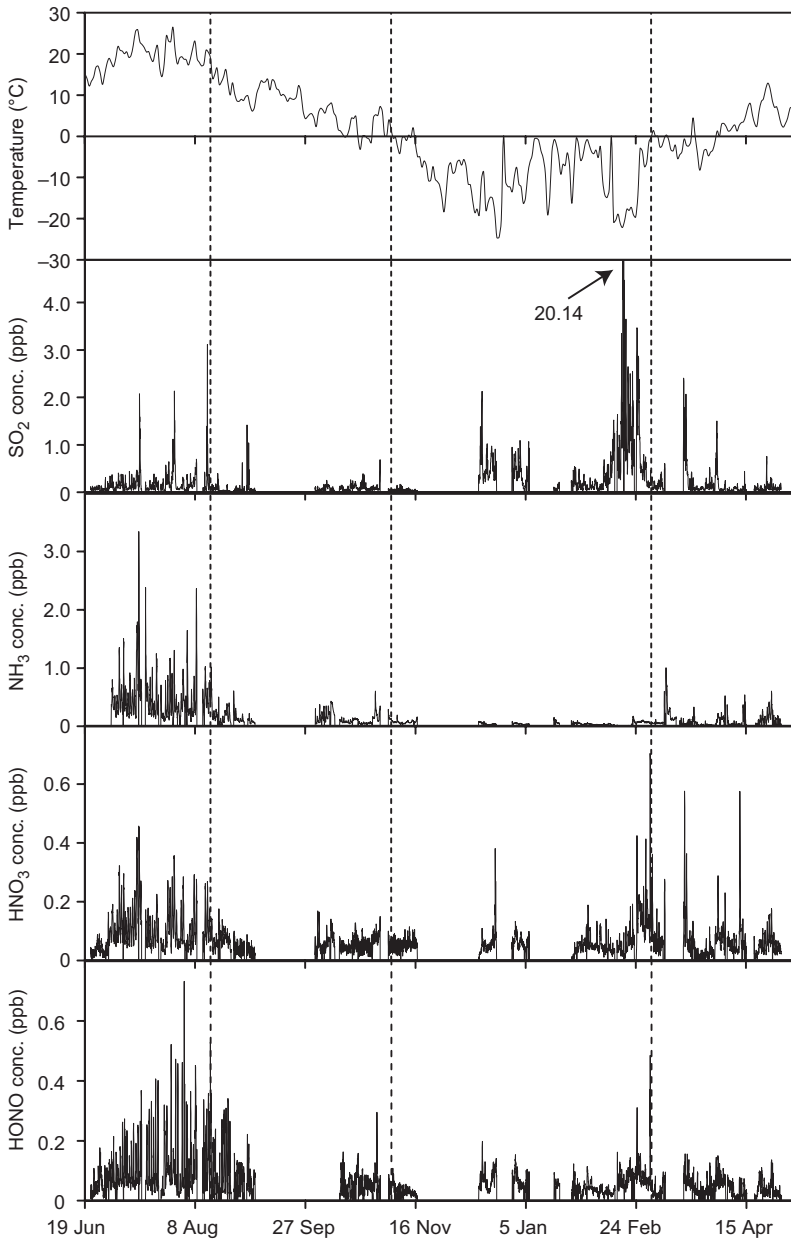


Fig. 4. Hourly-averaged temperature and gas concentrations at Hyytiälä from 22 June 2010 to 30 April 2011.

highest in summer and decreased towards winter, increasing again in spring (Fig. 4), following the temperature profile of the same period. During the coldest months when temperature was below 0 °C and the land was covered with snow, ammonia concentrations remained near the detection limit (the winter NH_3 average 0.05 ppb, NH_4^+ $0.38 \mu\text{g m}^{-3}$). In summer and autumn, the average ammonia concentrations were higher (0.47

and 0.13 ppb, respectively) than concentrations of the acidic gases SO_2 (0.18 and 0.08 ppb), HONO (0.11 and 0.07 ppb) and HNO_3 (0.10 and 0.06 ppb). Due to lower acid concentrations and warmer weather, ammonia was partitioned more to the gas phase in summer than in winter when there was an excess of acidic gases. A similar seasonal variation can be seen at all northern EMEP-stations where NH_3 is being measured using the

filter method, as well as in Canada (Zbieranowski and Aherne 2012). The main reason for the seasonal variation is that the agricultural sources of NH_3 are lower during the cold period. In Finland, agricultural outdoor activities normally start in May, leading to increased ammonia concentrations (Ruoho-Airola *et al.* 2010). In addition, at lower temperatures ammonia and nitric acid are usually in the form of ammonium nitrate, while at higher temperatures ammonium nitrate particles are easily volatilized according to $\text{NH}_3 + \text{HNO}_3 \leftrightarrow \text{NH}_4\text{NO}_3$.

In the aerosol phase, ammonium sulfate and nitrate, which are typical long-range transported species, were the most abundant compounds, and NH_4^+ concentration followed the profiles of SO_4^{2-} and NO_3^- (Fig. 6). Because the vapor pressure of ammonia over an acidic ammonium sulphate is much lower than that over ammonium

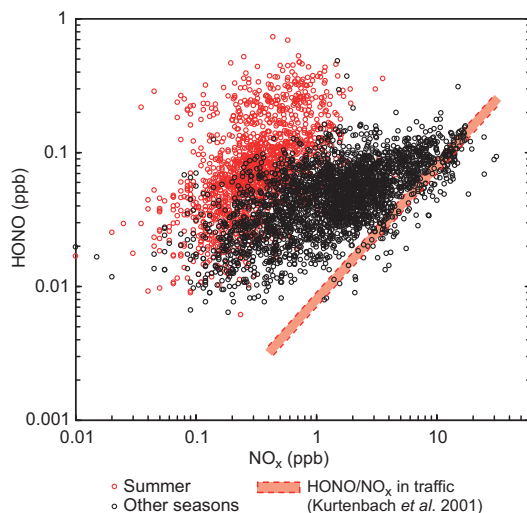


Fig. 5. Nitrous acid as a function of NO_x in summer and in the other seasons. The shaded red line shows the HONO-to- NO_x ratios 0.008 ± 0.001 found by Kurtenbach *et al.* (2001) in road traffic.

Table 2. Statistical summary of the trace gas data measured with MARGA at SMEAR II on 22 June 2010–30 April 2011. n = number of valid hourly results, n_{tot} = total number of hours in the period. Hydrochloric acid concentrations were not included as they were below the detection limit for most of the time and even 95% of values were below 0.04 ppb.

	Mean \pm SD (ppb)	Percentiles (ppb)			n/n_{tot}
		5	50	95	
All data					
HONO	0.07 \pm 0.06	0.02	0.05	0.19	4396/7422
SO_2	0.25 \pm 0.58	0.03	0.10	0.95	4736/7422
HNO_3	0.07 \pm 0.06	0.02	0.06	0.19	4665/7422
NH_3	0.18 \pm 0.24	0.02	0.08	0.63	4323/7422
Summer					
HONO	0.11 \pm 0.09	0.02	0.07	0.31	1145/1331
SO_2	0.18 \pm 0.24	0.04	0.11	0.50	1159/1331
HNO_3	0.10 \pm 0.07	0.03	0.08	0.25	1156/1331
NH_3	0.47 \pm 0.36	0.15	0.36	1.18	942/1331
Autumn					
HONO	0.07 \pm 0.05	0.02	0.06	0.19	844/1967
SO_2	0.08 \pm 0.09	0.02	0.06	0.18	1083/1967
HNO_3	0.06 \pm 0.03	0.02	0.05	0.10	1085/1967
NH_3	0.13 \pm 0.09	0.04	0.11	0.33	1063/1967
Winter					
HONO	0.06 \pm 0.03	0.02	0.05	0.11	1457/2832
SO_2	0.49 \pm 0.94	0.03	0.24	1.69	1483/2832
HNO_3	0.07 \pm 0.05	0.02	0.05	0.17	1433/2832
NH_3	0.05 \pm 0.03	0.02	0.05	0.10	1394/2832
Spring					
HONO	0.05 \pm 0.03	0.01	0.04	0.10	950/1392
SO_2	0.16 \pm 0.26	0.03	0.09	0.58	1011/1392
HNO_3	0.06 \pm 0.06	0.02	0.05	0.16	991/1392
NH_3	0.11 \pm 0.11	0.02	0.07	0.33	924/1392

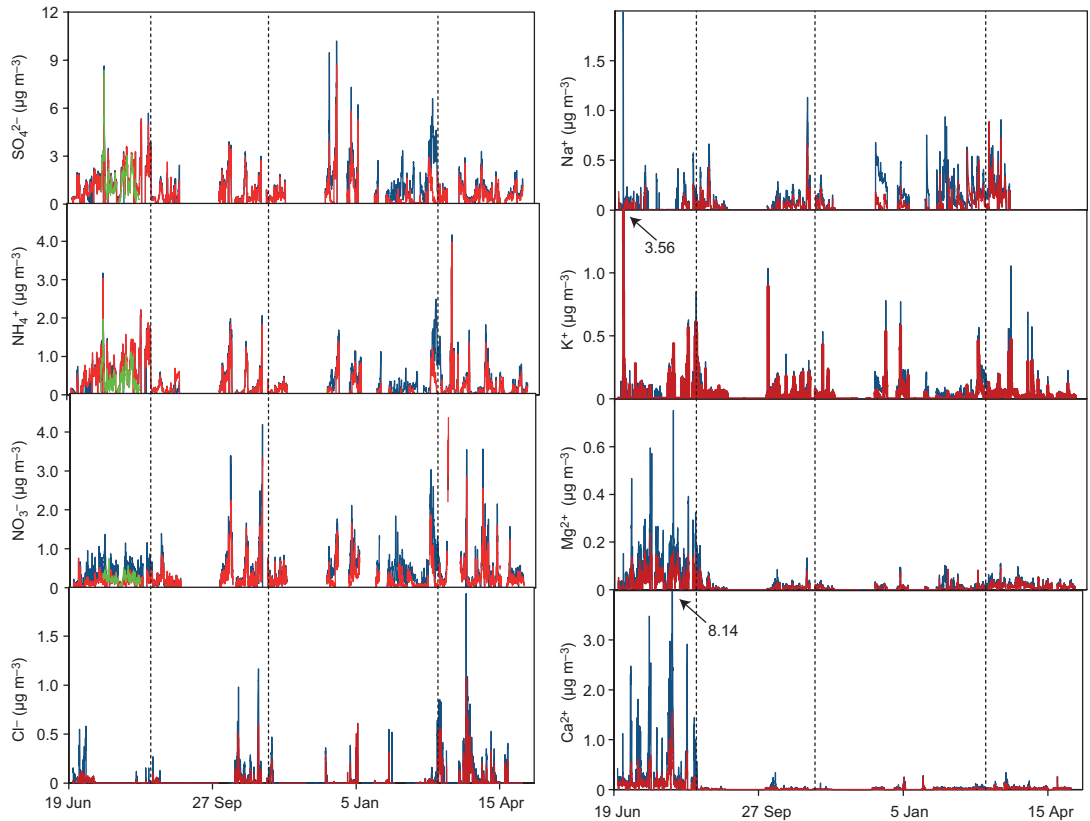


Fig. 6. Hourly-averaged concentrations of inorganic ions in $PM_{2.5}$ (red) and PM_{10} (blue) at Hyytiälä from 22 June 2010 to 30 April 2011. AMS data (cut-off $\sim 1 \mu\text{m}$) are presented in green.

nitrate, excess of ammonia leads to formation of ammonium nitrate, while the excess of acid sulphates leads to decomposition of ammonium nitrate (Ferm *et al.* 2012).

Concentrations of potassium, magnesium and calcium were very low in winter and spring (averages $0.02\text{--}0.07 \mu\text{g m}^{-3}$; Table 3). The highest concentration of potassium ($2.6 \mu\text{g m}^{-3}$ in $PM_{2.5}$ and $3.6 \mu\text{g m}^{-3}$ in PM_{10}) occurred on 25 June 2010, caused by the traditional Midsummer bonfires. Simultaneously, magnesium, calcium, sulphate and nitrate concentrations were elevated. On 1 January 2011, the fireworks of the New Year celebration caused K^+ , Mg^{2+} , Na^+ , Cl^- and SO_4^{2-} peaks (Fig. 6).

Diurnal cycles of nitrogen-containing gases

Nitric acid (HNO_3) is formed in the reaction NO_2

+ $\text{OH}\cdot + \text{M} \rightarrow \text{HNO}_3 + \text{M}$, where the hydroxyl radical $\text{OH}\cdot$ is formed in photochemical reactions in sunlight (Finlayson-Pitts and Pitts 2000). This is in agreement with our observations: in summer there was a clear diurnal cycle, with the maximum reached in the afternoon at 14:00–18:00 (Fig. 7). However, the peak concentration was observed several hours later than expected, since OH -radicals producing HNO_3 from NO_2 reached their highest concentrations at noon (Petäjä *et al.* 2009).

Nitrous acid HONO is formed in the reaction $\text{NO} + \text{OH}\cdot + \text{M} \rightarrow \text{HONO} + \text{M}$ and dissociated by solar radiation: $\text{HONO} + h\nu \rightarrow \text{OH}\cdot + \text{NO}$ (Finlayson-Pitts and Pitts 2000). Concentrations of HONO are thus higher at night and lower in sunlight. In Hyytiälä, the diurnal variation of the HONO concentrations was negligible during winter and also very modest during spring. As discussed above, the HONO -to- NO_x ratios suggest that a significant fraction of the recorded

HONO had been emitted from the soil. These data do not explain whether there was also a diurnal cycle in the emission rate or whether the cycle was only due to photochemistry.

In summer, the diurnal variation of the ammonia concentration was large, with a maximum in the afternoon (Fig. 8). At the same time, there was no diurnal cycle for particulate ammonium. Therefore, the summertime diurnal cycle of ammonia cannot be explained by the dissociation of NH_4NO_3 to NH_3 and HNO_3 . In winter, the ammonia concentration remained very low for most of the time, mainly below 0.1 ppb. In March there was no diurnal variation, but the variation in the concentrations as a whole was strong, with a maximum concentration of about 1 ppb. From the end of April the diurnal variation in ammonia began again.

Temperature dependence of ammonia concentrations

The observed diurnal cycle of the ammonia concentration suggests that ammonia previously absorbed on the leaf surfaces of trees and vegetation during the nighttime may be re-emitted as the temperature of the leaves rises again during warm summer days. In addition, decomposition

of leaves and processes within the forest soil releases ammonia. However, the simultaneous increase in VOC concentrations at the same site (Hakola *et al.* 2012) may indicate that biogenic ammonia sources also contribute.

Vegetation emits ammonia when exposed to air in which the ammonia concentrations are lower than the compensation point (denoted generally by χ_s), i.e., the ammonia partial pressure in the substomatal cavities of the plants (e.g. Farquhar *et al.* 1980). The reverse also occurs: if the atmospheric concentration is higher than the compensation point the plants act as a sink for ammonia. The ambient concentrations approach the compensation point when there are no additional ammonia sources or sinks (e.g. Langford and Fehsenfeld 1992). The compensation point depends on the temperature (e.g. Farquhar *et al.* 1980), ammonium concentration and pH in the plant apoplast, and these things depend on other factors such as the plant species and nitrogen supply (e.g. Schjoerring *et al.* 1998, Köstner *et al.* 2008).

The measurements discussed in the present paper are insufficient to determine the compensation point; for that measurement of fluxes would also be necessary. However, the observed temperature dependence is compared with that presented in the previous studies (Fig. 9). Lang-

Table 3. Statistical summary for the inorganic compounds measured in PM_{10} and $\text{PM}_{2.5}$ with the MARGA at SMEAR II on 22 June 2010–30 April 2011. Concentrations are given in $\mu\text{g m}^{-3}$ at 20 °C and 1013 hPa.

		All		Summer		Autumn		Winter		Spring	
		mean \pm SD	max	mean \pm SD	max	mean \pm SD	max	mean \pm SD	max	mean \pm SD	max
Cl ⁻	PM _{2.5}	0.04 \pm 0.10	1.08	0.02 \pm 0.02	0.13	0.05 \pm 0.10	0.60	0.02 \pm 0.07	0.61	0.08 \pm 0.14	1.08
	PM ₁₀	0.08 \pm 0.16	1.94	0.05 \pm 0.10	0.58	0.09 \pm 0.17	1.17	0.04 \pm 0.11	0.84	0.14 \pm 0.21	1.94
NO ₃ ⁻	PM _{2.5}	0.26 \pm 0.33	4.37	0.17 \pm 0.11	0.76	0.31 \pm 0.38	3.33	0.24 \pm 0.30	1.88	0.34 \pm 0.44	4.37
	PM ₁₀	0.41 \pm 0.45	4.19	0.33 \pm 0.23	1.37	0.38 \pm 0.53	4.19	0.47 \pm 0.45	3.03	0.44 \pm 0.54	3.89
SO ₄ ²⁻	PM _{2.5}	0.83 \pm 0.87	8.69	1.42 \pm 0.96	7.97	0.71 \pm 0.69	3.70	0.64 \pm 0.92	8.69	0.57 \pm 0.40	2.56
	PM ₁₀	1.08 \pm 1.07	10.20	1.34 \pm 1.02	8.64	0.77 \pm 0.76	3.91	1.39 \pm 1.38	10.20	0.70 \pm 0.49	3.30
Na ⁺	PM _{2.5}	0.06 \pm 0.09	0.89	0.02 \pm 0.04	0.26	0.06 \pm 0.09	0.67	0.07 \pm 0.09	0.89	0.20 \pm 0.12	0.72
	PM ₁₀	0.13 \pm 0.15	1.13	0.05 \pm 0.09	0.57	0.10 \pm 0.14	1.13	0.19 \pm 0.15	0.94	0.25 \pm 0.16	0.91
NH ₄ ⁺	PM _{2.5}	0.33 \pm 0.39	3.98	0.60 \pm 0.45	3.04	0.27 \pm 0.32	1.85	0.20 \pm 0.26	1.41	0.23 \pm 0.37	3.98
	PM ₁₀	0.37 \pm 0.43	4.17	0.55 \pm 0.47	3.17	0.27 \pm 0.35	2.07	0.38 \pm 0.43	2.49	0.28 \pm 0.41	4.17
K ⁺	PM _{2.5}	0.04 \pm 0.08	2.63	0.05 \pm 0.14	2.63	0.04 \pm 0.05	0.90	0.04 \pm 0.06	0.58	0.04 \pm 0.05	0.48
	PM ₁₀	0.06 \pm 0.10	3.56	0.07 \pm 0.17	3.56	0.05 \pm 0.06	1.04	0.07 \pm 0.08	0.78	0.04 \pm 0.07	1.06
Mg ²⁺	PM _{2.5}	0.02 \pm 0.03	0.24	0.05 \pm 0.04	0.24	0.01 \pm 0.01	0.09	0.01 \pm 0.01	0.09	0.02 \pm 0.01	0.09
	PM ₁₀	0.04 \pm 0.06	0.75	0.10 \pm 0.09	0.75	0.02 \pm 0.02	0.19	0.02 \pm 0.01	0.10	0.02 \pm 0.01	0.11
Ca ²⁺	PM _{2.5}	0.06 \pm 0.12	1.55	0.18 \pm 0.20	1.55	0.01 \pm 0.01	0.08	0.02 \pm 0.02	0.25	0.03 \pm 0.02	0.25
	PM ₁₀	0.13 \pm 0.38	8.14	0.47 \pm 0.68	8.14	0.02 \pm 0.03	0.34	0.03 \pm 0.03	0.28	0.03 \pm 0.03	0.34

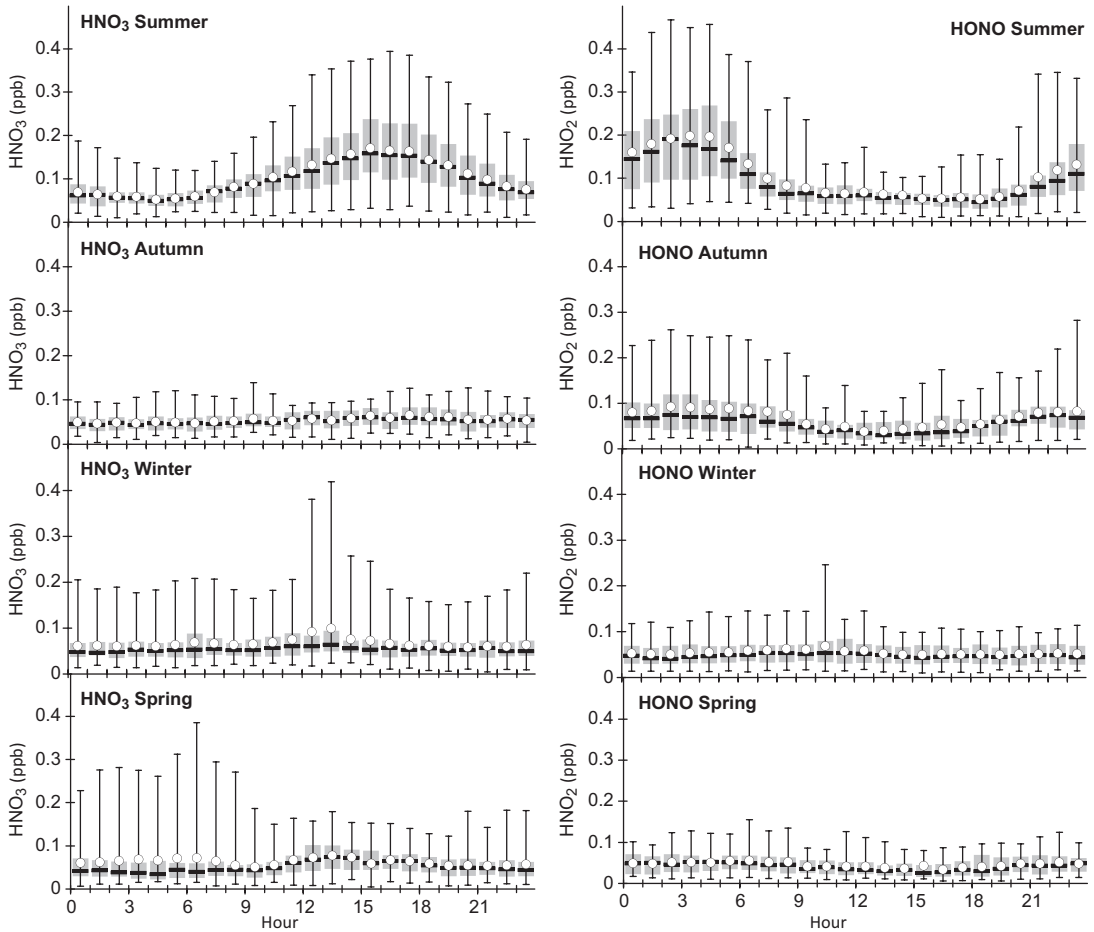


Fig. 7. Diurnal cycles of nitric and nitrous acids in the four seasons. The box represents the 25th to 75th percentile range, the bars the 90 percent range (5th and 95th percentiles), the horizontal line the median and the circle the averages of the hourly-averaged data for each hour.

ford and Fehsenfeld (1992) measured ammonia concentrations in a forest in Colorado and found that the compensation point was 0.8 ppb at 20 °C (cf. Fig. 9). The temperature-dependent compensation point χ_s was calculated from the formula (Husted and Schjoerring 1996, Tarnay et al. 2001):

$$\chi_s = \chi_s^* \exp \left[- \frac{\Delta H_{\text{dis}}^0 + \Delta H_{\text{vap}}^0}{R} \left(\frac{1}{T} - \frac{1}{T^*} \right) \right], \quad (1)$$

where χ_s^* is the compensation point at the temperature T^* , ΔH_{dis}^0 is the enthalpy of NH_4^+ dissociation = 52.21 kJ mol⁻¹, ΔH_{vap}^0 is the enthalpy of vaporization = 34.18 kJ mol⁻¹, $R = 8.314$ J mol⁻¹ K⁻¹, and T is the absolute temperature (cf. Fig. 9). Another approach is to measure the

compensation point of selected plant species. Köstner et al. (2008) used the results of Hartmann (2005) to calculate the stomatal ammonia compensation point of Norway spruce (*Picea abies*) needles and used the temperature dependence presented by Nemitz et al. (2000)

$$\chi_s = \frac{161500}{T} \exp \left(- \frac{10380}{T} \right) \frac{[\text{NH}_4^+]}{[\text{H}^+]}, \quad (2)$$

where $[\text{NH}_4^+]$ and $[\text{H}^+]$ are the ammonium and hydrogen ion concentrations, respectively, in the apoplast of the needles. At 25 °C the range of the compensation point was 0.11–0.27 ppb (Köstner et al. 2008; cf. Fig. 9).

These concentrations are higher than those determined only from the needles but lower than

the compensation point in the forest in Colorado. A probable explanation is that the measured ammonia is emitted not only by Norway spruce but also by other vegetation around the measurement site. Further studies would be needed to determine the ammonia compensation points of various species at SMEAR II.

The data presented in Fig. 9 were further used for deriving a function describing the temperature dependence of ammonia. It is not called the compensation point here, since the measurements were insufficient to determine whether the ammonia concentration was in equilibrium. An exponential function of temperature fitted to all the data yielded the function

$$[\text{NH}_3](T) = [\text{NH}_3]_0 \exp(kT) \\ = 0.077(\text{ppb})\exp[0.071T(^{\circ}\text{C})]. \quad (3)$$

Next, the data were grouped into relative humidity ranges, and an exponential function $[\text{NH}_3] = [\text{NH}_3]_0 \exp(kT)$ was again fitted to the data (Fig. 9). The factors k and $[\text{NH}_3]_0$ varied almost linearly with the relative humidity, RH (Fig. 10). These factors were combined, yielding the function

$$[\text{NH}_3](\text{RH}, T) = \\ = [0.000739(\text{ppb}) \text{RH}(\%) + 00891(\text{ppb})] \\ \times \exp[(-0.00118\text{RH} + 0.164)T(^{\circ}\text{C})]. \quad (4)$$

The concentrations modelled with the functions given by Eqs. 3 and 4 were plotted against the measurements (Fig. 11). The function given by Eq. 3, which takes only temperature into account, clearly agrees less with the data than the function given by Eq. 4, which depends on RH as well. Even though the coefficients of determination ($r^2 = 0.631$ and $r^2 = 0.644$) are approximately the same, the function given by Eq. 4 yields concentrations much closer to the 1:1 line, especially at the higher concentrations. However, it is obvious from the scatter in the data that even if both RH and temperature are taken into account, the differences between the modelled and observed concentrations are still large, showing that ammonia concentrations depend strongly on other factors too. This parameterization needs to be quantified and verified with detailed emission measurements.

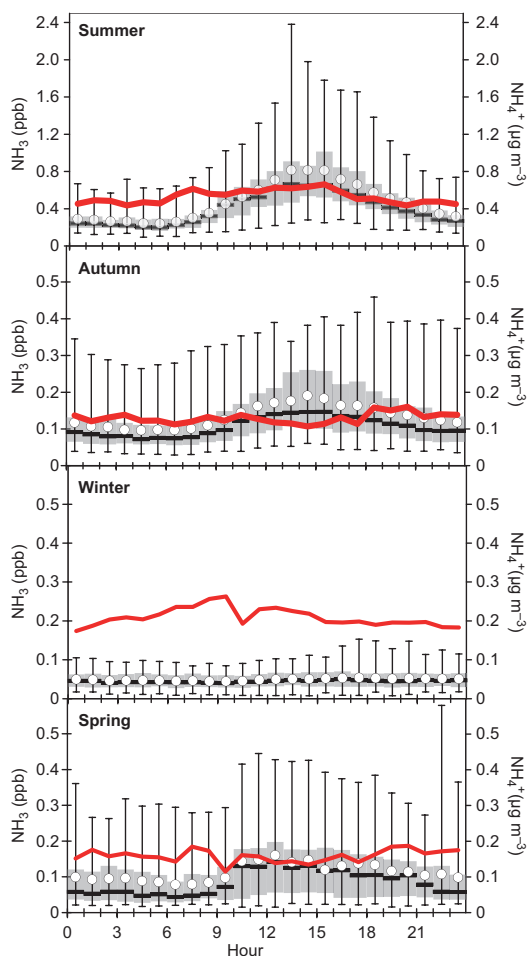


Fig. 8. Diurnal cycle of ammonia in the four seasons. The box represents the 25th to 75th percentile range, the bars the 90% range (5th and 95th percentiles), the horizontal line the median and the circle the averages of the hourly-averaged data for each hour. The red lines present the medium ammonium concentrations ($\mu\text{g m}^{-3}$) in PM_{10} fraction.

The temperature dependence found in this study is in agreement with earlier findings. Warm weather leads to greater ammonia volatilization (Monteny and Erisman 1998) and also increases emissions from vegetation. An increase in the temperature from 15 to 30 °C may cause a plant to switch from being a strong sink for atmospheric NH_3 to being a significant NH_3 source (Schoerring *et al.* 1998). Husted and Schoerring (1996) found that increasing the leaf temperatures of oilseed rape plants from 10 to 35 °C caused an exponential increase in NH_3 emission

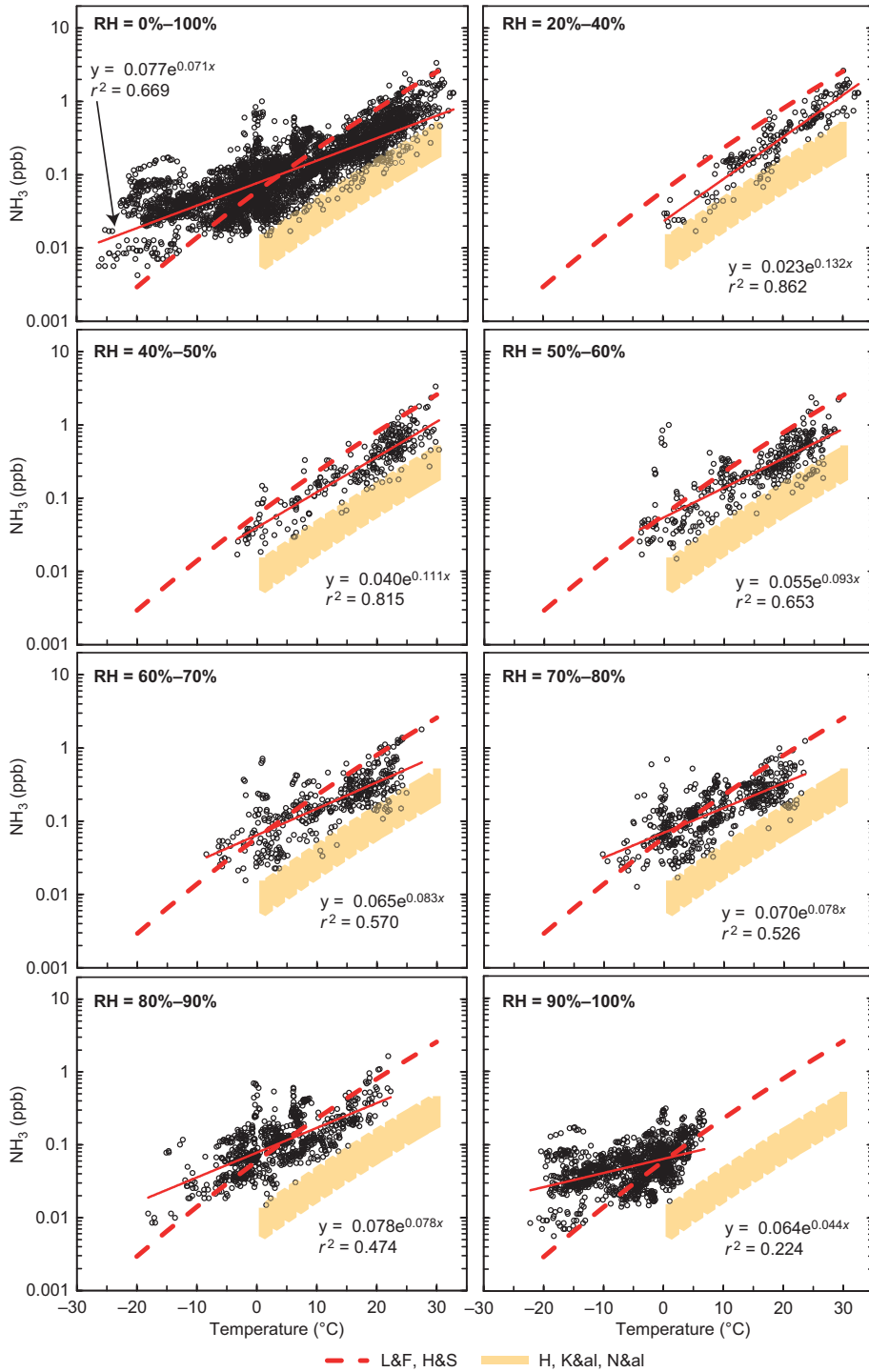


Fig. 9. Ammonia concentration as a function of temperature in eight ranges of relative humidity (red, solid line; this work). The dashed, red line shows the ammonia compensation point determined from measurements in a forest in Colorado by Langford and Fehsenfeld (1992: L&F) and by using the temperature dependence calculated with the formula presented by Husted and Schjoerring (1996: H&S), and the yellow shaded area the range of ammonia compensation points of Norway Spruce needles determined by Hartmann (2005: H) and Köstner *et al.* (2008: K&al) with the temperature dependence presented by Nemitz *et al.* (2000: N&al).

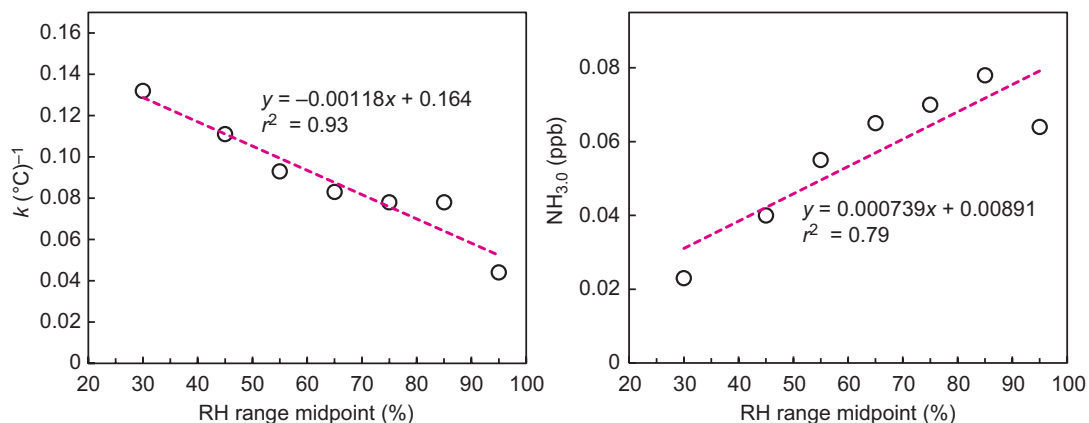


Fig. 10. Variation of the factors k and $[\text{NH}_3]_0$ in $[\text{NH}_3] = [\text{NH}_3]_0 \exp(k \times T(^{\circ}\text{C}))$ and $[\text{NH}_3]_0$ as a function of RH range midpoint, as obtained from the exponential fits in Fig. 9.

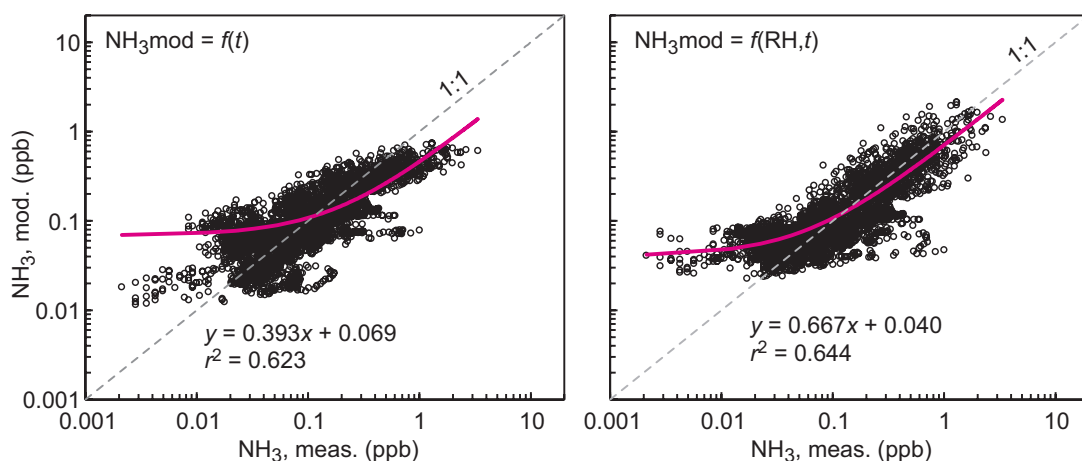


Fig. 11. Comparison of modelled and measured ammonia concentrations. In the left-hand-side panel the modelled concentrations were calculated with Eq. 3, and in the right-hand-side panel with Eq. 4. In both plots the red line is the linear regression described by the equation.

from plants exposed to low ambient NH_3 concentrations.

Conclusions

In this study, we presented for the first time, concentrations of ionic compounds in particulate matter and ammonia measured with a 1-h time resolution at a Nordic background site. The results of this study suggest that the EMEP filter method could indeed be replaced with a MARGA instrument equipped with a concentration column, at least for cations. This would reduce the laboratory work, e.g. the pretreatment

of filters, but it would increase the maintenance work in the field. On the other hand, there would be several benefits from using data with 1-h time resolution instead of daily-average results, such as monitoring of diurnal profiles and their seasonal cycles and other short-term variability, which is not possible with the traditional filter methods. Gas and aerosol data with a higher time resolution could also be used for model evaluations (Schaap 2011) and for various kinds of atmospheric chemistry or aerosol studies, for example for getting detailed information on the gas-aerosol partitioning of semi-volatile species. When compared with those produced by AMS, satisfactory results were achieved for sulphate

and ammonium, but for nitrate there was a large variation because of the different cutoff.

All the compounds measured with MARGA agreed quite well with the concentrations obtained from the analyses of the EMEP filter pack, except for nitric acid. The concentrations of HNO_3 measured with MARGA were only about 50% of those found on the impregnated filter. For a better recovery of HNO_3 in the MARGA system, short Teflon inlet-tubing should be used, as recommended by Rumsay *et al.* (2013), bearing in mind that it may also disturb the collection of particulate matter. In parallel measurements of cavity ring-down spectroscopy (CRDS) and of the MARGA instrument in Kleiner Feldberg in Germany, elevated nocturnal concentrations of N_2O_5 led to nighttime peaks in the HNO_3 concentrations measured by MARGA (Phillips *et al.* 2013). However, in Hyytiälä we could not find any nighttime HNO_3 peaks that indicated the presence of N_2O_5 .

The average concentrations of all nitrogen-containing gases were highest in summer when both HONO and HNO_3 showed diurnal cycles depending on the amount of sunlight. In summer, the HONO concentrations were clearly higher than those predicted by a ratio of HONO to NO_x concentrations in road traffic emissions alone, suggesting that soil is a source of HONO in summer. This is in line with the findings of Su *et al.* (2011). Ammonia also showed a clear diurnal cycle in the summer, with a maximum at noon, but during cold periods (temperature below 0 °C) ammonia concentrations were often below the detection limit. In spring the diurnal variation of ammonia started again.

Ammonia concentrations were exponentially dependent on the prevailing temperature, in line with published temperature dependence of ammonia compensation points. The concentration was lower than that calculated from data presented from a forest in Colorado, but higher than that calculated from the compensation point of Norway spruce needles. The increase with temperature was greater during drier periods. For particulate ammonium there was no diurnal cycle, so the daily variation of ammonia was most likely caused by emissions, something that needs to be studied further.

Acknowledgements: This work was supported by the Academy of Finland as part of the Centre of Excellence program (project no. 1118615).

References

- Aan de Brugh J.M.J., Henzing J.S., Schaap M., Morgan W.T., van Heerwaarden C.C., Weijers E.P., Coe H. & Krol M.C. 2012. Modelling the partitioning of ammonium nitrate in the convective boundary layer. *Atmos. Chem. Phys.* 12: 3005–3023.
- Bouwman A.F., Lee D.S., Asman W.A.H., Dentener F.J., Van Der Hoek K.W. & Olivier J.G.J. 1997. A global high-resolution emission inventory for ammonia. *Global Biogeochem. Cycles* 11: 561–587.
- Butterbach-Bahl K., Nemitz E., Zaehle S., Billen B., Boeckx P., Erismann J.W., Garnier J., Upstill-Goddard R., Kreuzer M., Oenema M., Reis S., Schaap M., Simpson D., de Vries W., Winiwarter W. & Sutton M.A. 2011. Nitrogen as a threat to the European greenhouse balance. In: Sutton M.A., Howard C., Erismann J.W., Billen G., Bleeker A., Grennfelt P., van Grinsven H. & Grizzetti B. (eds.), *The European nitrogen assessment: sources, effects and policy perspectives*, Cambridge University Press, Cambridge, pp. 434–462.
- Cape J.N. 2009. *Operation of EMEP 'supersites' in the United Kingdom. Annual report for 2007*. Available at http://nora.nerc.ac.uk/8660/2/EMEP_supersite_report_2007N008660OCR.pdf.
- Draxler R.R. & Rolph G.D. 2013. *HYSPLIT (Hybrid Single-Particle Lagrangian Integrated Trajectory) Model*. NOAA Air Resources Laboratory, College Park, MD. [Available at <http://www.arl.noaa.gov/HYSPLIT.php>].
- Drewnick F., Hings S.S., DeCarlo P.F., Jayne J.T., Gonin M., Fuhrer K., Weimer S., Jimenez J.L., Demerjian K.L., Borrmann S. & Worsnop D.R. 2005. A new Time-of-Flight Aerosol Mass Spectrometer (ToF-AMS) — instrument description and first field deployment. *Aerosol Sci. Technol.* 39: 637–658.
- EMEP 2001. *EMEP manual for sampling and chemical analysis*. EMEP/CCC-Report 1/95, Rev. 2001, Norwegian Institute for Air Research, Kjeller. [Available at <http://www.nilu.no/projects/ccc/manual/index.html>].
- Farquhar G.D., Firth P.M., Wetselaar R. & Weir B. 1980. On the gaseous exchange of ammonia between leaves and the environment. Determination of the ammonia compensation point. *Plant Physiology* 66: 710–714.
- Ferm M. & Hellsten S. 2012. Trends in atmospheric ammonia and particulate ammonium concentrations in Sweden and its causes. *Atmos. Environ.* 60: 30–39.
- Finlayson-Pitts B.J. & Pitts J.N. 2000. *Chemistry of the upper and lower atmosphere: theory, experiments and application*. Academic Press, San Diego, CA.
- Hakola H., Hellén H., Hemmilä M., Rinne J. & Kulmala M. 2012. In situ measurements of volatile organic compounds in a boreal forest. *Atmos. Chem. Phys.* 12: 11665–11678.
- Hari P. & Kulmala M. 2005. Station for measuring ecosys-

- tem-atmosphere relations (SMEAR II). *Boreal Env. Res.* 10: 315–322.
- Hartmann A. 2005. *Erarbeitung von Methoden zur Extraktion der Extrazellulärflüssigkeit von Fichtennadeln für die Bestimmung des Ammoniak-Kompensationspunktes*. Diploma Thesis, Interdisziplinäres Ökologisches Zentrum, TU Bergakademie Freiberg.
- Husted S. & Schjoerring J.K. 1996. Ammonia flux between oilseed rape plants and the atmosphere in response to changes in leaf temperature, light intensity, and air humidity — interactions with leaf conductance and apoplastic NH_4^+ and H^+ concentrations. *Plant Physiology* 112: 67–74.
- Jayne J.T., Leard D.C., Zhang X., Davidovits P., Smith K.A., Kolb C.E. & Worsnop D.R. 2000. Development of an aerosol mass spectrometer for size and composition analysis of submicron particles. *Aerosol Sci. Technol.* 33: 49–70.
- Jimenez J.L., Jayne J.T., Shi Q., Kolb C.E., Worsnop D.R., Yourshaw I., Seinfeld J.H., Flagan R.C., Zhang X., Smith K.A., Morris J.W. & Davidovits P. 2003. Ambient aerosol sampling using the Aerodyne Aerosol Mass Spectrometer. *J. Geophys. Res.* 108(D7), 8425, doi:10.1029/2001JD001213.
- Khlystov A., Wyers G.P. & Slanina J. 1995. The steam-jet aerosol collector. *Atmos. Environ.* 29: 2229–2234.
- Kirkby J., Curtius J., Almeida I., Dunne E., Duplissy J., Ehrhart S., Franchin A., Gagné S., Ickes L., Kürten A., Kupc A., Metzger A., Riccobono F., Rondo L., Schobesberger S., Tsagkogeorgas G., Wimmer D., Amorim A., Bianchi F., Breitenlechner M., David A., Dommen J., Downard A., Ehn M., Flagan R.C., Haider S., Hansel A., Hauser D., Jud W., Junninen H., Kreissl F., Kvashin A., Laaksonen A., Lehtipalo K., Lima J., Lovejoy E.R., Makhmutov V., Mathot S., Mikkilä J., Minginette P., Mogo S., Nieminen T., Onnela A., Pereira P., Petäjä T., Schnitzhofer R., Seinfeld J.H., Sipilä M., Stozhkov Y., Stratmann F., Tomé A., Vanhanen J., Viisanen Y., Vrtala A., Wagner P.E., Walther H., Weingartner E., Wex H., Winkler P.M., Carslaw K.S., Worsnop D.R., Baltensperger U. & Kulmala M. 2011. Role of sulphuric acid, ammonia and galactic cosmic rays in atmospheric aerosol nucleation. *Nature* 476: 429–433.
- Köstner B., Matyssek R., Heilmeyer H., Clausnitzer F., Nunn A.J. & Wieser G. 2007. Sap flow measurements as a basis for assessing trace-gas exchange of trees. *Flora* 203: 14–33.
- Kulmala M. & Petäjä T. 2011. Soil nitrites influence atmospheric chemistry. *Science* 333: 1586–1587.
- Kulmala M., Pirjola L. & Mäkelä J.M. 2000. Stable sulphate clusters as a source of new atmospheric particles. *Nature* 404: 66–69.
- Langford A.O. & Fehsenfeld F.C. 1992. Natural vegetation as a source or sink for atmospheric ammonia: a case study. *Science* 255: 581–583.
- Liu P.S.K., Deng R., Smith K.A., Williams L.R., Jayne J.T., Canagaratna M.R., Moore K., Onasch T.B., Worsnop D.R. & Deshler T. 2007. Transmission efficiency of an aerodynamic focusing lens system: comparison of model calculations and laboratory measurements for the Aerodyne Aerosol Mass spectrometer. *Aerosol Sci. Technol.* 41: 721–733.
- Makkonen U., Virkkula A., Mäntykonttä J., Hakola H., Keronen P., Vakkari V. & Aalto P.P. 2012. Semi-continuous gas and inorganic aerosol measurements at a Finnish urban site: comparisons with filters, nitrogen in aerosol and gas phases, and aerosol acidity. *Atmos. Chem. Phys.* 12: 5617–5631.
- Monteny G.J. & Erisman J.W. 1998. Ammonia emission from dairy cow buildings: a review of measurement techniques, influencing factors and possibilities for reduction. *Netherlands Journal of Agricultural Science* 46: 225–247.
- Neuman J.A., Huey L.G., Ryerson T.B. & Fahey D.W. 1999. Study of inlet materials for sampling atmospheric nitric acid. *Environ. Sci. Technol.* 33: 1133–1136.
- Nemitz E., Sutton M.A., Schjoerring J.K., Husted S. & Wyers G.P. 2000. Resistance modelling of ammonia exchange over oilseed rape. *Agric. For. Meteorol.* 105: 405–425.
- Park J. & Lin M.C. 1997. A mass spectrometric study of the $\text{NH}_2 + \text{NO}_2$ reaction. *J. Phys. Chem. A* 101: 2643–2647.
- Petäjä T., Mauldin R.L.III, Kosciuch E., McGrath J., Nieminen T., Paasonen P., Boy M., Adamov A., Kotiaho T. & Kulmala M. 2009. Sulphuric acid and OH concentrations in a boreal forest site. *Atmos. Chem. Phys.* 9: 7435–7448.
- Phillips G.J., Makkonen U., Schuster G., Sobanski N., Hakola H. & Crowley J.N. 2013. The detection of nocturnal N_2O_5 as HNO_3 by alkali- and aqueous-denuder techniques. *Atmos. Meas. Tech.* 6: 231–237.
- Rolph G.D. 2013. *Real-time Environmental Applications and Display sYstem (READY)*. NOAA Air Resources Laboratory, College Park, MD. [Available at <http://www.ready.noaa.gov>].
- Rumsey I.C., Cowen K.A., Walker J.T., Kelly T.J., Hanft E.A., Mishoe K., Rogers C., Proost R., Beachley G.M., Lear G., Frelink T. & Otjes R.P. 2013. An assessment of the performance of the Monitor for AeRosols and GAses in ambient air (MARGA): a semi-continuous method for soluble compounds. *Atmos. Chem. Phys. Discuss.* 13: 25067–25124.
- Ruoho-Airola T., Leppänen S. & Makkonen U. 2010. Changes in the concentration of reduced nitrogen in the air in Finland between 1990 and 2007. *Boreal Env. Res.* 15: 427–436.
- Schaap M., Otjes R.P. & Weijers E.P. 2011. Illustrating the benefit of using hourly monitoring data on secondary inorganic aerosol and its precursors for model evaluation. *Atmos. Chem. Phys.* 11: 11041–11053.
- Schjoerring J.K., Husted S. & Mattsson M. 1998. Physiological parameters controlling plant-atmosphere ammonia exchange. *Atmos. Environ.* 32: 491–498.
- Slanina J., ten Brink H.M., Otjes R.P., Even A., Jongejan P., Khlystov S., Waijers-Ijpelaan A., Hu M. & Lu Y. 2001. The continuous analysis of nitrate and ammonium in aerosols by the steam jet aerosol collector (SJAC): extension and validation of the methodology. *Atmos. Environ.* 35: 2319–2330.
- Su H., Cheng Y., Oswald R., Behrendt T., Trebs I., Meixner F., Andreae M., Cheng P., Zhang Y. & Pöschl U. 2011. Soil nitrite as a source of atmospheric HONO and OH

- radicals. *Science* 333: 1616–1618.
- Sutton M.A., Howard C., Erisman J.W., Billen G., Bleeker A., Grennfelt P., van Grinsven H. & Grizzetti B. 2011a. *The European nitrogen assessment*. Cambridge University Press, Cambridge.
- Sutton M.A., Nemitz E., Skiba U.M., Beier C., Butterbach-Bahl K., Cellier P., de Vries W., Erisman J.W., Reis S., Bleeker A., Bergamaschi P., Calanca P.L., Dalgaard T., Duyzer J., Gundersen P., Hensen A., Kros J., Leip A., Olesen J.E., Owen S., Rees R.M., Sheppard L.J., Smith P., Zechmeister-Boltenstern S., Soussana J.F., Theobald M.R., Twigg M., van Oijen M., Veldkamp T., Vesala T., Winiwarter W., Carter M.S., Dragosits U., Flechard C., Helfter C., Kitzler B., Rahn K.H., Reinds G.J. & Schleppi P. with contributions from the NitroEurope community 2011b. *The nitrogen cycle and its influence on the European greenhouse gas balance*. Centre for Ecology and Hydrology.
- Tarnay L., Gertler A.W., Blank R.R. & Taylor G.E.Jr. 2001. Preliminary measurements of summer nitric acid and ammonia concentrations in the Lake Tahoe Basin airshed: Implications for dry deposition of atmospheric nitrogen. *Environ. Pollut.* 113: 145–153.
- ten Brink H.M., Otjes R., Jongejan P. & Slanina S. 2007. An instrument for semi-continuous monitoring of the size-distribution of nitrate, ammonium, sulphate and chloride in aerosol. *Atmos. Environ.* 41: 2768–2779.
- Williams J., Crowley J., Fischer H., Harder H., Martinez M., Petäjä T., Rinne J., Bäck J., Boy M., Dal Maso M., Hakala J., Kajos M., Keronen P., Rantala P., Aalto J., Aaltonen H., Paatero J., Vesala T., Hakola H., Levula J., Pohja T., Herrmann F., Auld J., Mesarchaki E., Song W., Yassaa N., Nölscher A., Johnson A.M., Custer T., Sinha V., Thieser J., Pouvesle N., Taraborrelli D., Tang M.J., Bozem H., Hosaynali-Beygi Z., Axinte R., Oswald R., Novelli A., Kubistin D., Hens K., Javed U., Trawny K., Breitenberger C., Hidalgo P.J., Ebben C.J., Geiger F.M., Corrigan A.L., Russell L.M., Ouwersloot H.G., Vilà-Guerau de Arellano J., Ganzeveld L., Vogel A., Beck M., Bayerle A., Kampf C.J., Bertelmann M., Köllner F., Hoffmann T., Valverde J., González D., Riekkola M.-L., Kulmala M. & Lelieveld J. 2011. The summertime Boreal forest field measurement intensive HUMPPA-COPEC-2010: an overview of meteorological and chemical influences. *Atmos. Chem. Phys.* 11: 10599–10618.
- Zbieranowski A.L. & Aherne J. 2012. Spatial and temporal concentration of ambient atmospheric ammonia in southern Ontario, Canada. *Atmos. Environ.* 62: 441–450.